Simple synthesis of three primary colour nanoparticle inks of Prussian blue and its analogues

Akihito Gotoh[1]**, Hiroaki Uchida**[1]**, Manabu Ishizaki**[1]**,
Tetsutaro Satoh**[1]**, Shinichi Kaga**[1]**, Shusuke Okamoto**[1]**,
Masaki Ohta**[1]**, Masatomi Sakamoto**[1,2]**, Tohru Kawamoto**[2]**,
Hisashi Tanaka**[2]**, Madoka Tokumoto**[2,3]**, Shigeo Hara**[2]**,
Hirofumi Shiozaki**[2]**, Mami Yamada**[4]**, Mikio Miyake**[5] **and
Masato Kurihara**[1,2,6]

[1] Department of Material and Biological Chemistry, Faculty of Science, Yamagata University,
1-4-12 Kojirakawa-machi, Yamagata 990-8560, Japan
[2] Nanotechnology Research Institute, National Institute of Advanced Industrial Science and
Technology (AIST), 1-1-1 Umezono, Tsukuba 305-8568, Japan
[3] Department of Applied Physics, National Defense Academy, 1-10-20 Hashirimizu,
Yokosuka, Kanagawa 239-8686, Japan
[4] Tokyo University of Agriculture and Technology, 2-24-16 Nakamachi, Koganei,
Tokoyo 184-8588, Japan
[5] Advanced Institute of Science and Technology (JAIST), Asahidani 1-1, Nomi,
Ishikawa 923-1292, Japan

E-mail: kurihara@sci.kj.yamagata-u.ac.jp

Abstract
Historic Prussian blue (PB) pigment is easily obtained as an insoluble
precipitate in quantitative yield from an aqueous mixture of Fe^{3+} and
$[Fe^{II}(CN)_6]^{4-}$ (Fe^{2+} and $[Fe^{III}(CN)_6]^{3-}$). It has been found that the PB
pigment is inherently an agglomerate of 10–20 nm nanoparticles, based on
powder x-ray diffraction (XRD) line broadenings and transmission electron
microscopy (TEM) images. The PB pigment has been revived as both
organic-solvent-soluble and water-soluble nanoparticle inks. Through crystal
surface modification with aliphatic amines, the nanoparticles are stably
dispersed from the insoluble agglomerate into usual organic solvents to
afford a transparent blue solution. Identical modification with $[Fe(CN)_6]^{4-}$
yields water-soluble PB nanoparticles. A similar ink preparation is applicable
to Ni-PBA and Co-PBA (nickel and cobalt hexacyanoferrates). The PB
(blue), Ni-PBA (yellow), and Co-PBA (red) nanoparticles function as three
primary colour inks.

S Supplementary data are available from stacks.iop.org/Nano/18/345609

1. Introduction

Prussian blue (PB = iron hexacyanoferrate) pigment, with its three-century history, is recognized as the first synthetic coordination compound, which presents a remarkable blue colour. It is derived from the charge transfer (CT) of the mixed valence state (Fe(II)–CN–Fe(III)) around 700 nm with a large molar extinction coefficient ($\sim$$10^4$ M^{-1} cm^{-1}) [1]. Multi-functionalities of PB and its analogues (PBAs) have recently renewed scientific as well as industrial interests, such as electrochromic displays [2–5], electrocatalysts [6], secondary batteries [7, 8], ion- and bio-sensors [9–12],

[6] Author to whom any correspondence should be addressed.

photo-magnets [13], and hydrogen storage [14, 15]. The PB pigment is easily obtained as an insoluble precipitate in quantitative yield from an aqueous mixture of Fe^{3+} and $[Fe^{II}(CN)_6]^{4-}$ (Fe^{2+} and $[Fe^{III}(CN)_6]^{3-}$). However, insolubility in common solvents is such a salient demerit that direct manipulation of the pigment for practical functional electronic devices has been discontinued. Consequently, the functional applications of PB (and PBAs) have remained limited to electrodeposited films in many cases. A method is needed to disperse PB into a solvent as nanoparticles, creating a nanoparticle ink, for the development of new PB-based devices that can be designed with fine patterns or films using advanced printing techniques, e.g., ink-jet printing.

Although PB is one of the most studied coordination compounds, it is a long-standing question why the PB pigment is insoluble in most common solvents. Recently, it has been understood that the so-called 'insoluble PB', $Fe_4[Fe(CN)_6]_3 \cdot x H_2O$, is a bulk solid, and nanoscience has also presented a new field related to the syntheses of PB and PBA nanoparticles during the last seven years [16–18]. In fact, reversed micelle [19–28], polymer-protection [29–34], and template [35–37] syntheses effectively inhibit the crystal growth of PB and PBAs. Moreover, their sufficiently small nanoparticles are allowed to be soluble (dispersed) in various organic solvents. Water-soluble PB nanoparticles have also been developed for applications as electrochromic displays [2, 38]. However, the industrial applications of these soluble PB and PBA nanoparticles would necessitate changing their costly and complicated synthetic procedures.

Herein we reveal that the PB pigment is inherently an insoluble agglomerate of 10–20 nm nanoparticles, but not a bulk solid. We report on the crystal surface modification of the nanoparticles, providing a low-cost, efficient, and simple production method for both organic-solvent-soluble and water-soluble (dispersible) PB nanoparticle inks. Through surface modification with aliphatic amines, the nanoparticles are stably redispersed from the insoluble agglomerates into usual organic solvents. Identical modification with $[Fe(CN)_6]^{4-}$ yields water-soluble PB nanoparticles. A similar ink preparation is applicable to Ni-PBA and Co-PBA (nickel and cobalt hexacyanoferrates).

2. Experimental details

2.1. Materials

$Fe(NO_3)_3 \cdot 9H_2O$, $Ni(NO_3)_2 \cdot 6H_2O$, $Na_4[Fe(CN)_6] \cdot 10H_2O$, $K_3[Fe(CN)_6]$, and ammonia water (28–30%) were purchased as extra pure grades from Kanto Chemicals. $Co(CH_3COO)_2 \cdot 4H_2O$ and $(NH_4)_4[Fe(CN)_6] \cdot H_2O$ were supplied from Woko Chemicals (as an extra pure grade) and Johnson Matthey Company, respectively. All reagents to prepare the PB pigment and Ni- and Co-PBAs were used without further purification. Oleylamine was used as received from Tokyo Chemical Industry to prepare the PB and PBAs nanoparticle inks.

2.2. Synthesis of PB pigment

An aqueous solution (30 ml) of $Fe(NO_3)_3 \cdot 9H_2O$ (16.2 g, 40.1 mmol) was added to an aqueous solution (60 ml)

of $Na_4[Fe(CN)_6] \cdot 10H_2O$ (14.5 g, 30.0 mmol) or $(NH_4)_4[Fe(CN)_6] \cdot H_2O$ (9.06 g, 30.0 mmol). The reaction mixture was vigorously stirred for 5 min. The resulting blue precipitate was centrifuged, washed with water three times and with methanol once, and then dried under reduced pressure to yield the insoluble PB pigment as $Fe_4[Fe(CN)_6]_3 \cdot 15H_2O$ (11.0 g, 97.4%), where the hydration number was determined by a thermogravimetric/differential thermal analysis (TG/DTA; Shimadzu DTG-60).

2.3. Synthesis of organic solvent-dispersible PB nanoparticle ink

The insoluble PB pigment (1.00 g, 0.885 mmol) was suspended in toluene (15 ml) containing water (2 ml). Into the suspension, oleylamine (0.650 g, 2.43 mmol) was added and stirred for 1 h at room temperature. During the reaction period, the PB solid almost disappeared and was eluted into the toluene layer as a deep-blue solution, in which the transformation reaction was accelerated by the addition of water. The reaction mixture was dehydrated with anhydrous Na_2SO_4 and filtered through a celite layer. The PB pigment was almost fully recovered as a deep-blue solution but there was a little loss due to adsorbed blue components on the celite. After evaporation of the resulting transparent blue solution to dryness, the obtained solid residue can be redissolved in the usual organic solvents ($\geqslant 0.1$ g (PB) ml^{-1} in toluene). In preparation of the organic solvent-dispersible PB nanoparticles, the synthetic solvent, toluene, can be reduced to the minimum volume (2.0 ml) to enable agitation of the PB pigment (1.0 g) with oleylamine (0.65 g).

2.4. Synthesis of water-dispersible PB nanoparticle ink

The insoluble PB pigment (0.40 g, 0.35 mmol) was suspended in water (8 ml). Into the suspension, $Na_4[Fe(CN)_6] \cdot 10H_2O$ (60–480 mg, 0.12–0.992 mmol) was added and stirred for 0.5–30 h at room temperature; the reaction time depended on the amount of the ferrocyanide ion. During the reaction period, the suspension completely changed into a transparent deep-blue solution without any PB solids. The solution was filtered and, after evaporation to dryness, the obtained solid residue can be redissolved into water ($\geqslant 0.1$ g (PB) ml^{-1}) and methanol.

2.5. Synthesis of Ni-PBA

An aqueous solution (30 ml) of $Ni(NO_3)_2 \cdot 6H_2O$ (8.72 g, 30.0 mmol) was added to an aqueous solution (30 ml) of $K_3[Fe(CN)_6]$ (6.59 g, 20.0 mmol). The reaction mixture was vigorously stirred for 5 min. The precipitated Ni-PBA, $K_{0.14}Ni_{1.43}[Fe(CN)_6] \cdot 5H_2O$, was separated in a similar procedure to the PB pigment in the yield of 9.0 g, where the hydration number was determined by the TG/DTA analysis and the metal composition ratio was Fe:Ni = 1:1.43 according to the fluorescent x-ray analysis (Rigaku Primini, WDX). The metal composition ratio slightly deviates from the ideal ratio of Fe:Ni = 1:1.5 ($Ni_{1.5}[Fe(CN)_6]$) and the deficient positive charge is compensated by potassium ions.

2.6. Synthesis of Co-PBA

An aqueous solution (10 ml) of $Co(CH_3COO)_2 \cdot 4H_2O$ (0.63 g, 2.5 mmol) was added to an aqueous solution (8 ml) of $K_3[Fe(CN)_6]$ (0.83 g, 2.5 mmol) and ammonia water (28–30%, 0.34 ml). The reaction mixture was vigorously stirred for 3 min. The precipitated Co-PBA, $K_{0.1}Co_{1.45}[Fe(CN)_6] \cdot 5.5H_2O \cdot NH_3$, was separated in a similar procedure to the PB pigment in the yield of 0.83 g, where the number of water and ammonia molecules was based on the elemental analyses (wt%): C, 17.03 (calculated 17.26); H, 3.32 (3.38); N, 23.03 (23.49) and the metal composition ratio was Fe:Co = 1:1.45 according to the fluorescent x-ray analysis. The metal composition ratio slightly deviates from the ideal ratio of Fe:Co = 1:1.5 ($Co_{1.5}[Fe(CN)_6]$) and the deficient positive charge is compensated by potassium ions.

2.7. Synthesis of PBA nanoparticle inks

The Ni-PBA and Co-PBA nanoparticle inks were prepared similarly to the toluene-dispersible PB nanoparticle ink.

2.8. Measurements

Powder x-ray diffraction (XRD) analyses were performed using a Rigaku Rint 2000 x-ray diffractometer (Cu Kα_1 radiation). Transmission electron microscopy (TEM) images of the PB and PBA nanoparticles were observed using a JEOL JEM-2000EX transmission electron microscope. Ultraviolet–visible (UV–vis) absorption spectra of the PB and PBA nanoparticle inks were recorded on a Shimadzu MultiSpec-1500 spectrometer. The dynamic light-scattering (DLS) particle sizes and zeta potentials of the PB nanoparticles were measured on an Otsuka ELS-Z2M zeta-potential and particle size analyser. The charge transfer of the PB nanoparticles absorbs laser light (660 nm); therefore, the zeta potentials were only measured in the dilute methanol dispersion. From the dilute aqueous dispersions reproducible and steady zeta potentials were obtained unsuccessfully, as they were negative values.

3. Results and discussion

According to recent discoveries of PB and PBA nanoparticles with dimensions ranging from several nanometres to over several hundred nanometres, the mean particle size estimated from the line widths of powder x-ray diffraction (XRD) signals by Scherrer's equation is consistent with that from transmission electron microscopy (TEM) images. The XRD line widths of the submicrocrystals are quite narrow [26, 39], but the particles of several-nanometre and several-tens-of-nanometre scale show considerably broad XRD signals [27–29, 40]. The insoluble PB pigment obtained using the common synthetic method exhibited notably broad XRD signals (figure 1(a)). The XRD broadening was reproduced in our reiterated syntheses and previously reported syntheses [29, 41]. The mean particle size is estimated as ~13 nm on the basis of Scherrer's equation. Although the insoluble PB pigment is believed to be a bulk solid, it should be considered as an aggregated solid of much smaller nanoparticles. In fact, TEM images have revealed that
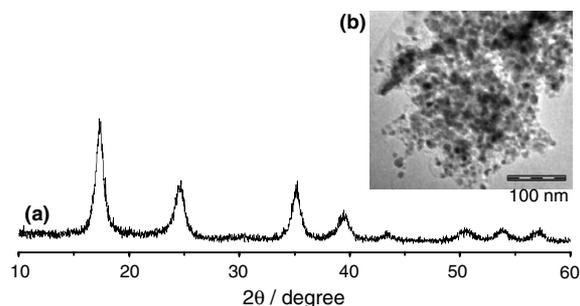
Figure 1. XRD pattern (a) and TEM image (b) of the insoluble PB pigment. The insoluble PB pigment is suspended with acetone. The suspension is placed on a TEM microgrid.

the PB pigment is an aggregated form of nanoparticles of 10–20 nm dimensions (figure 1(b)). We deduce that innumerable PB nanoparticles appear at once through the rapid coordination reaction, in which both reactants, Fe^{3+} and $[Fe(CN)_6]^{4-}$, are immediately consumed from the reaction solution. In the case of water-soluble PB, $KFe[Fe(CN)_6] \cdot xH_2O$, the negative surface charge attributable to the partial dissociation of K^+ prevents the precipitation caused by the mutual aggregation of its nanoparticles [2]. The neutral surface charge of the insoluble PB facilitates the aggregation precipitation even in much smaller nanoparticles. Under such common reaction conditions, the critical particle size that leads to aggregation precipitation is less than 20 nm (figure 1(b)), although crystal growth can proceed at submicrometre [39] or submillimetre [42] sizes in special cases, decelerating the coordination reaction.

Each nanoparticle can be redispersed into various solvents by displacement of the water ligands of $Fe(III)–OH_2$ sites on the crystal surfaces [27, 28] if the PB pigment insolubility arises from a simple physical aggregation of nanoparticles. Using this synthetic strategy (figure 2), two kinds of PB nanoparticle ink, i.e., organic-solvent-soluble and water-soluble (dispersible) PB nanoparticles, were prepared from the insoluble PB pigment.

In one attempt to revive the PB pigment as nanoparticle inks with organic solvents, the PB pigment was stirred with oleylamine in toluene (figure 2(a)). The suspension was almost entirely transformed into a deep-blue transparent solution. A residue after evaporation of the filtrate exhibits unaltered XRD line widths, suggesting that the nanoparticle size is maintained in the dispersion reaction (figure S1 (available at stacks.iop.org/Nano/18/345609)). The PB nanoparticles can be stably redispersed from the residue in many organic solvents, such as toluene, hexane, chloroform, diethylether, and *n*-butylacetate, but not in methanol, to provide a blue nanoparticle ink of an arbitrary PB concentration (maximum concentration ⩾0.1 g (PB) ml^{-1} in toluene). The 10–20 nm nanoparticles in the toluene dispersion solution were confirmed from a TEM image (figure 3(a)). In the UV–vis absorption spectrum of a dilute dispersion solution of the PB nanoparticles (figure 4(a)), the intense band at 676 nm is due to CT from Fe(II) to Fe(III) [29].

The behaviour of the secondary aggregation of the nanoparticles via interaction between aliphatic chains on the crystal surface was investigated using different C_{18}-amines.
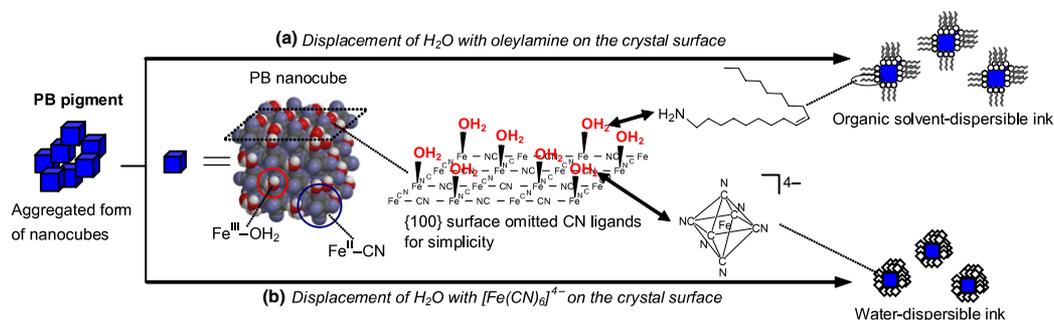
Figure 2. Preparation of PB nanoparticle inks from the insoluble PB pigment using surface Fe(III)–OH$_2$ moieties. The PB nanoparticles are shown as an ideal cubic shape (nanocube) surrounded by six {100} surfaces, which consist of a 4 × 4 arrangement of irons with a 0.5 nm × 3 dimension. The 10 and 20 nm nanocubes are, respectively, three-dimensional 21 × 21 × 21 and 41 × 41 × 41 structures. In an ideal 10–20 nm PB nanocube, the surface Fe(III)–H$_2$O sites occupy 7.5–15%, numerically, of all Fe ions. (a) The PB pigment was exposed in organic solvents to 25–40% of oleylamine, numerically, of all Fe ions. (b) The PB pigment was exposed in water to 5–40% of Na$_4$[Fe(CN)$_6$], numerically, of all Fe ions.
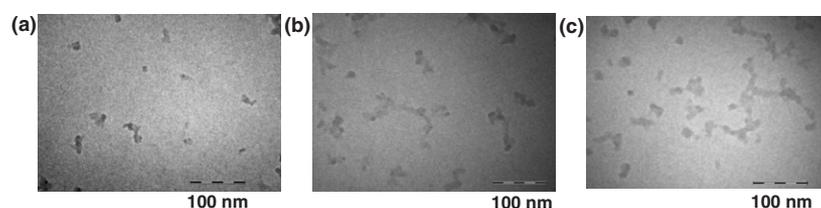
Figure 3. TEM images of (a) PB, (b) Ni-PBA, and (c) Co-PBA nanoparticles in the toluene-dispersible inks.
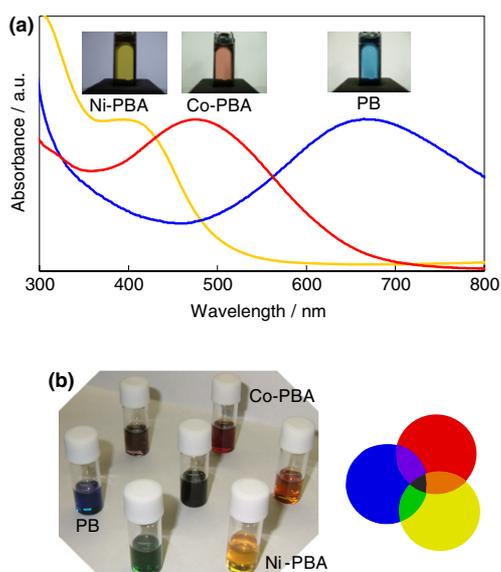
Figure 4. (a) UV–vis absorption spectra of the PB (blue line), Co-PBA (red line), and Ni-PBA (yellow line) nanoparticles in their transparent dilute toluene dispersion. (b) Hue circle produced by dichromatic tuning of the three inks. The trichromatic mixture of PB, Ni-PBA, and Co-PBA nanoparticle inks exhibits a black colour (centre of the hue circle).

In toluene, PB nanoparticles treated with octadecylamine are precipitated at around 5 °C, but the nanoparticles are redispersed with an increase in temperature up to 30 °C. Interestingly, oleylamines maintain the dispersed state of the

PB nanoparticles down to −10 °C. This fact indicates that the nanoparticles are separated from one another through surface modification with these aliphatic amines. Aggregation of the nanoparticles is more effectively inhibited by the bent C$_{18}$-*cis*-chain, CH$_3$(CH$_2$)$_7$CH=CH(CH$_2$)$_8$NH$_2$, of oleylamine than by the straight chain of octadecylamine. The particle size should be evaluated even in transparent dispersion solutions for the use of the nanoparticle ink, especially in ink-jet printing. From a possible high-concentration toluene-dispersion solution of the oleylamine-modified PB nanoparticles (28 mg (PB) ml^{-1}) for dynamic light-scattering (DLS) measurements [40], the number-averaged particle size is estimated as 15 ± 2 nm at 25 °C (figure 5(a)), which is consistent with the primary particle size. The oleylamine-modified nanoparticles can be stably dispersed without secondary aggregation. The oleylamine-modified nanoparticle ink is suitable for fabrication of PB-based electronic devices using the fine printing techniques.

As another attempt to produce a water-dispersible nanoparticle ink, the PB pigment was subjected to a similar surface modification using ferrocyanide anions, [Fe(CN)$_6$]$^{4−}$ (figure 2(b)). An aqueous suspension of the PB pigment was completely transformed into a deep-blue transparent solution merely by agitation with 15% ferrocyanide ions of the total number of Fe ions of the PB pigment. The number-averaged particle size is 21 ± 6 nm from the DLS measurement of a high-concentration water-dispersible PB ink (25 mg ml^{-1}) at 25 °C (figure 5(b)). The DLS number-averaged particle size is practically independent of the amount of the added ferrocyanide ion (5–40%), which is near the primary particle size. On the other hand, the DLS size distribution is wider than that of the toluene-dispersible nanoparticles
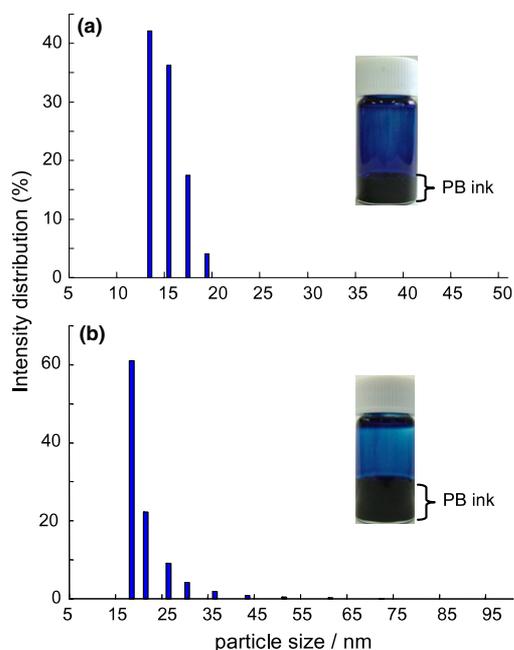
Figure 5. DLS number-averaged particle-size distribution.
(a) a high-concentration toluene-dispersible PB ink.
(b) a high-concentration water-dispersible PB ink.

(figure 5), suggesting that the PB nanoparticles are stably dispersed in water as primary particles and their aggregated forms, observed from a TEM image (figure S2 (available at stacks.iop.org/Nano/18/345609)). Solid residues obtained by evaporation of the transparent blue aqueous solutions show the unaltered XRD line width and the mean particle size ranges between 11 and 13 nm, based on Scherrer's equation. XRD signals attributable to the unreacted sodium ferrocyanide are detected in cases of addition of 20% or more. The signals intensify as the sodium ferrocyanide content increases (figure S3 (available at stacks.iop.org/Nano/18/345609)). This observation indicates that the surface unsaturated coordination sites, Fe(III)–OH$_2$, occupy 15–20% of the total number of Fe ions of PB and the occupancy corresponds to PB nanoparticles of 7.5–10 nm, based on a cubic model without roughness of the crystal surface (figure 2). The PB nanoparticles can be stably redispersed in water from all the solid residues as arbitrary concentration inks (maximum concentration ⩾0.1 g (PB) ml^{-1}). Solids with 7–15% ferrocyanide ions are most dispersible in methanol. The maximum concentration is ∼35 mg ml^{-1}, while the solubility decreases with increasing the ferrocyanide ion concentration (>20%). The zeta potentials of the PB nanoparticles in the dilute methanol dispersion were measured as a negative value, which is −23 mV in the case of a nearly saturated crystal surface with the ferrocyanide ion (15%). These results indicate that replacement of the water ligands with [Fe^{II}(CN)$_6$]$^{4-}$ occurs in the open coordination space on the crystal surface (figure 2(b)) and each nanoparticle has a negative surface charge (a negative zeta potential). That surface charge prevents the PB nanoparticles from their insoluble aggregation.

A similar nanoparticle ink can be prepared from the insoluble precipitates of nickel and cobalt hexacyanoferrates (Ni-PBA and Co-PBA) with a general formula M$_{1.5}$[Fe(CN)$_6$] (M = Co and Ni). The XRD analysis of the precipitates shows that the mean particle size is small: PB (13 nm) ⩽ Ni-PBA (14) < Co-PBA (18) (figure S4 (available at stacks.iop.org/Nano/18/345609)). The precipitates are agglomerates of nanoparticles, as confirmed from the TEM images (figure S5 (available at stacks.iop.org/Nano/18/345609)). We attempted the transformation of the insoluble PBAs into their organic solvent-dispersible inks using oleylamine. The insoluble Ni-PBA was almost eluted as 10–20 nm nanoparticles into toluene to provide a transparent yellow ink (figures 3(b) and 4(a)). The Co-PBA precipitate was also transformed into a transparent red ink composed of 10–20 nm nanoparticles (figures 3(c) and 4(a)). The PB, Co-PBA, and Ni-PBA nanoparticles operate as three primary colour inks. The dichromatic tuning of the three inks affords a hue circle containing green, orange, and purple (figure 4(b)). These colour inks will be applicable to an electrochromic indicator and matrix display fabricated using advanced printing techniques.

4. Conclusion

It should be emphasized that the PB pigment was, in fact, an insoluble aggregated form of nanoparticles (much smaller colloidal particles) before the recent discovery of the individually separated nanoparticles [16–18]. Our method for the synthesis of nanoparticle ink controls the insoluble aggregation state of nanoparticles from the historic PB pigment, differing from recent preparations of dispersed nanoparticles [16–18]. Those preparations consume enormous amounts of organic solvents and surfactants or protecting agents. Furthermore, the variety of the utilizable synthetic solvents is limited, especially in the reversed micelle preparation. In contrast, our synthesis can use various organic solvents, which can be reduced to the minimum volume to enable agitation of the PB pigment with oleylamine. Our nanoparticle inks are most promising for future industrial use because they offer low cost, efficiency, simplicity, and applicability to mass production. The ancient pigment is still new as a nanomaterial even after 300 years from its discovery.

Acknowledgments

References

[1] Itaya K, Ataka T and Toshima S 1982 *J. Am. Chem. Soc.* **104** 4767
[2] DeLongchamp D M and Hammond P T 2004 *Adv. Funct. Mater.* **14** 224
[3] Tung T S and Ho K C 2006 *Sol. Energy Mater. Sol. Cells* **90** 521
[4] Varshney P, Deepa M, Agnihotry S A and Ho K C 2003 *Sol. Energy Mater. Sol. Cells* **79** 449
[5] de Tacconi N R, Rajeshwar K and Lezna R O 2003 *Chem. Mater.* **15** 3046

[6] Itaya K, Shoji N and Uchida I 1984 *J. Am. Chem. Soc.*
106 3423

[7] Eftekhari A 2004 *J. Power Sources* **132** 291

[8] Tung T S, Chen L C and Ho K C 2003 *Solid State Ion.* **165** 257

[9] Yang M, Jiang J, Yang Y, Chen X, Shen G and Yu R 2006
Biosens. Bioelectron. **21** 1791

[10] Zhao W, Xu J J, Shi C G and Chen H Y 2005 *Langmuir*
21 9630

[11] Fiorito P A, Gonçales V R, Ponzio E A and
de Torresi S I C 2005 *Chem. Commun.* **2005** 366

[12] Yuan R, Zhang L, Li Q, Chai Y and Cao S 2005 *Anal. Chim.
Acta* **531** 1

[13] Sato O, Hayami S, Einaga Y and Gu Z Z 2003 *Bull. Chem. Soc.
Japan* **76** 443

[14] Kaye S S and Long J R 2005 *J. Am. Chem. Soc.* **127** 6506

[15] Chapman K W, Southon P D, Weeks C L and Kepert C J 2005
Chem. Commun. **2005** 3322

[16] Uemura T and Kitagawa S 2005 *Chem. Lett.* **34** 132

[17] Dujardin E and Mann S 2004 *Adv. Mater.* **16** 1125

[18] Mann S, Davis S A, Hall S R, Li M, Rhodes K H, Shenton W,
Vaucher S and Zhang B 2000 *J. Chem. Soc., Dalton Trans.*
2000 3753

[19] Kondo N, Nakajima A, Sasaki Y, Kurihara M, Yamada M,
Miyake M, Mizukami F and Sakamoto M 2006 *Chem. Lett.*
35 1302

[20] Taguchi M, Yamada K, Suzuki K, Sato O and Einaga Y 2005
Chem. Mater. **17** 4554

[21] Kondo N, Kurihara M, Yamada M, Miyake M, Nishijima M,
Ohsuna T, Mizukami F and Sakamoto M 2005 *Chem. Lett.*
34 590

[22] Sun H L, Shi H, Zhao F, Qi L and Gao S 2005 *Chem. Commun.*
2005 4339

[23] Kondo N, Yokoyama A, Kurihara M, Sakamoto M, Yamada M,
Miyake M, Ohsuna T, Aono H and Sadaoka Y 2004 *Chem.
Lett.* **33** 1182

[24] Vaucher S, Fielden J, Li M, Dujardin E and Mann S 2002 *Nano
Lett.* **2** 225

[25] Vaucher S, Li M and Mann S 2000 *Angew. Chem. Int. Edn*
39 1793

[26] Cao M, Wu X, He X and Hu C 2005 *Chem. Commun.*
2005 2241

[27] Yamada M, Arai M, Kurihara M, Sakamoto M and
Miyake M 2004 *J. Am. Chem. Soc.* **126** 9482

[28] Catala L, Gacoin T, Boilot J P, Rivière É, Paulsen C,
Lhotel E and Mallah T 2003 *Adv. Mater.* **15** 826

[29] Uemura T, Ohba M and Kitagawa S 2004 *Inorg. Chem.*
43 7339

[30] Catala L, Gloter A, Stephan O, Rogez G and Mallah T 2006
Chem. Commun. **2006** 1018

[31] Kong Q, Chen X, Yao J and Xue D 2005 *Nanotechnology*
16 164

[32] Catala L, Mathonière C, Gloter A, Stephan O, Gacoin T,
Boilot J P and Mallah T 2005 *Chem. Commun.* **2005** 746

[33] Li Z, Zhang J, Mu T, Du J, Liu Z, Han B and Chen J 2004
Colloids Surf. A **243** 63

[34] Uemura T and Kitagawa S 2003 *J. Am. Chem. Soc.* **125** 7814

[35] Johansson A, Widenkvist E, Lu J, Boman M and
Jansson U 2005 *Nano Lett.* **5** 1603

[36] Gálvez N, Sánchez P and D-Vera J M 2005 *Dalton Trans.*
2005 2492

[37] D-Vera J M and Colacio E 2003 *Inorg. Chem.* **42** 6983

[38] Bocharova V *et al* 2006 *Progr. Colloid Polym. Sci.* **132** 161

[39] Wu X, Cao M, Hu C and He X 2006 *Crystal Growth Design*
6 26

[40] Bagkar N, Ganguly R, Choudhury S, Hassan P A, Sawant S and
Yakhmi J V 2004 *J. Mater. Chem.* **14** 1430

[41] Imanishi N, Morikawa T, Kondo J, Takeda Y, Yamamoto O,
Kinuagsa N and Yamagishi T 1999 *J. Power Sources* **79** 215

[42] Buser H J, Schwarzenbach D, Petter W and Ludi A 1977 *Inorg.
Chem.* **16** 2704